

A NON-LINEAR FILTERING APPROACH TO RIDGE AND FURROW SEGMENTATION OF FINGERPRINTS

I. O. A. Omeiza

Information Technology Laboratory, Department of Electrical Engineering,
University of Ilorin, P. M. B 1515, Ilorin, Nigeria.

ABSTRACT

Ridge and furrow segmentation or ridge extraction is an important processing step in automatic fingerprint identification; as its success simplifies the task of tracing the most distinguishing features of the print, the ridge ends and bifurcations. In this work a new method for ridge extraction in fingerprints is proposed. The method uses normalisation, local histogram equalisation, median filtering and global thresholding to segment the fingerprint foreground into ridges and furrows. The result obtained shows that the new algorithm is robust to image noise. It is also less computationally demanding when compared with an earlier ridge detection scheme.

Keywords: fingerprint, normalization, histogram equalisation, median filtering, ridge and furrow segmentation.

INTRODUCTION

In 1893, the Home Ministry Office, UK, accepted that no two individuals have the same fingerprints (Maltoni et. al, 2003). As such, fingerprint matching is one of the most reliable means of persons identification. Law enforcement agencies have effectively used it for criminal identification. Now, it is also being used in several other applications such as access control for high security installations, credit card usage verification, electronic voting, national ID card, and employee identification (Miller, 1994; Hong, 1998). However the manual matching of fingerprints is very inconvenient when the number of fingerprints or the database size is large. For the purpose of automation, a suitable representation (feature extraction) of fingerprints is essential (Ratha et. al, 1996).

Each fingerprint is a map of ridges and valleys (also known as furrows) in the epidermis layer of the skin at the finger tip. The ridge and valley structures form unique geometric patterns. A closer analysis of the fingerprint reveals that the ridges (or the valleys) exhibit anomalies of various kinds, such as ridge bifurcations and endings. The ridge endings and bifurcations are called minutiae, and these minutiae have a pattern that is unique to each finger (Jain et.al, 1997b). The directions of the ridges associated with minutiae, the relative positions of the minutiae and the number of ridges (or valleys) between any pair of minutiae are some of the features that uniquely characterise a fingerprint. Automated fingerprint identification or verification systems that use these features are

considered minutiae based. The vast majority of contemporary automated fingerprint identification or verification systems are minutiae-based systems.

Several approaches to automatic minutiae extraction have been proposed: Although rather different from one another, most of these methods transform fingerprint images into binary images through an ad hoc algorithm. The images obtained are then submitted to a thinning process which allows for the ridge-line thickness to be reduced to one pixel. Minutiae detection over the thinned image becomes a simple process. This is done by following the thinned ridges to locate bifurcations and terminations on the thinned image. The overall success of this approach lies heavily on the effective binarisation of the fingerprint foreground (ridge and furrow segmentation) as opposed to the original grey-level image. The general problem of image binarisation, sometimes referred to as segmentation, has been widely studied in the fields of image processing and pattern recognition (Pal and Pal, 1993). The easiest approach uses a global threshold 't', and works by setting to 0 the pixels whose grey level is lower than t and to 1 the remaining. The histograms of fingerprint images are not bimodal (Halici et.al, 1999). For that reason a global threshold is not sufficient for a correct segmentation. Local thresholding may be applied, except that grey-level image enhancement is a must in such an approach. In the specific case of fingerprint which are usually of poor quality, a local threshold method can not always guarantee acceptable results hence, ad hoc solutions exploiting specific knowledge of this application

domain have been proposed and summarised as follows.

Coetzee and Botha (1993) proposed a binarisation technique based on the use of edges in conjunction with the grey-scale image. Edge extraction is performed through Marr-Hildreth algorithm (1980). A sophisticated technique, which operates on small local window through a blob-colouring routine, allows the edge and intensity information to be fused. O’Gorman and Nickerson (1989) presented a technique for fingerprint enhancement and binarisation based on the convolution of the image with some filters oriented according to the directional or orientation image. The filters are computed parametrically with respect to the ridge-line characteristic at the resolution used: min. and max. ridge-line width, min. and max. ridge-line inter-distance, max. bending. This kind of filtering performs a local regularisation which is very robust with respect to noise, since it relies in directional information which can be reliably extracted even on poor images; but the method requires the convolution of each point with a large mask, resulting in a very time-consuming process (Maio and Maltoni, 1999).

Jain et. al. (1997b) proposed another method for ridges detection in which the input fingerprint is convolved with two masks, $h_t(i, j; u, v)$ and $h_b(i, j; u, v)$, of size $L \times H$ (on an average 11×7), respectively. These two masks are capable of adaptively accentuating the local maximum grey-level values along a direction normal to the local ridge direction.

$$h_t(i, j; u, v) = \begin{cases} -\frac{1}{\sqrt{2\pi\delta}} e^{-\frac{u^2}{2\delta}}, & \text{if } u = (v \cot(\theta(i, j))), \\ -\frac{H}{2 \cos(\theta(i, j))}, & v \in \Omega \end{cases} \quad (1)$$

$$\begin{cases} \frac{1}{\sqrt{2\pi\delta}} e^{-\frac{v^2}{2\delta}}, & \text{if } u = (v \cot(\theta(i, j))), \\ 0, & \text{otherwise} \end{cases} \quad v \in \Omega$$

$$h_b(i, j; u, v) = \begin{cases} -\frac{1}{\sqrt{2\pi\delta}} e^{-\frac{u^2}{2\delta}}, & \text{if } u = (v \cot(\theta(i, j))), \\ +\frac{H}{2 \cos(\theta(i, j))}, & v \in \Omega \end{cases} \quad (2)$$

$$\begin{cases} \frac{1}{\sqrt{2\pi\delta}} e^{-\frac{v^2}{2\delta}}, & \text{if } u = (v \cot(\theta(i, j))), \\ 0, & \text{otherwise} \end{cases} \quad v \in \Omega$$

$$\Omega = \left[-\left| \frac{L \sin(\theta(i, j))}{2} \right|, \left| \frac{L \sin(\theta(i, j))}{2} \right| \right] \quad (3)$$

where $\theta(i, j)$ represents the local ridge direction at pixel (i, j) and δ is a large constant. If both of the grey-level values at pixel (i, j) of the convolved images are larger than a certain threshold T_{ridge} , then pixel (i, j) is labeled as a ridge.

In this work a new approach to ridge and furrow segmentation of fingerprints is presented. The method differs from the previously reported ones, in that it focuses on the elimination of sweat-

pore details from the ridges. It uses a non-linear filter for smoothening as opposed to the use of large convolutional masks and it does not require the computation of orientation estimates in local neighbourhoods, a time consuming activity. As such the new algorithm is faster in execution. It also uses image normalisation and histogram equalisation as preprocessing steps.

In the following sections, the main steps of the ridge and furrow segmentation algorithm, and experimental results of this approach are discussed.

Normalisation

The input fingerprint image is normalised to constant mean and variance in order to remove the effect of varying or unequal finger pressure across the image. It is done using the following method, which is presented by Hong et. al. (1998).

Let $I(i, j)$ denote the grey level value at pixel (i, j) , M and VAR , the estimated mean and variance of the input fingerprint image respectively. If $N(i, j)$ denote the normalized grey-level value at pixel (i, j) , the normalised image is defined as follows

$$N(i, j) = \begin{cases} M_d + \sqrt{\frac{VAR_d \times (I(i, j) - M)^2}{VAR}} \\ M_d - \sqrt{\frac{VAR_d \times (I(i, j) - M)^2}{VAR}} \end{cases} \quad (4)$$

where M_d and VAR_d are the desired mean and variance values.

Histogram Equalisation

Histogram equalisation defines a mapping of grey levels r into grey levels s such that the distribution of grey levels s is uniform. This mapping stretches contrast for grey levels near the histogram maxima, and thus improves the detectability of many image features.

The grey levels in an image are random quantities in the normalized interval $(0,1)$. This enhancement technique is based on modifying the appearance of the image by controlling the probability density function of its grey levels via a transformation function $T(r)$ that satisfies the following conditions.

- (a) $T(r)$ is single – valued and monotonically increasing in the interval $0 \leq r \leq 1$
- (b) $0 \leq T(r) \leq 1$ for $0 \leq r \leq 1$

Assuming for a moment that they are continuous variables, the original and transformed grey-levels can be characterized by their probability density functions $P_r(r)$ and $P_s(s)$

A suitable $T(r)$ is given by

$$S = T(r) = \int_0^r P_r(w) dw \quad 0 \leq r \leq 1 \quad (5)$$

will be wrongly classified as valley pixels (see Fig.1b). It is to prevent this pitfall, that the new algorithm incorporates a nonlinear filter (a median filter) to eliminate the sweat pore details before thresholding. Fig.2b shows the result of application of median filtering alone to the specimen fingerprint reproduced as Fig.2a.

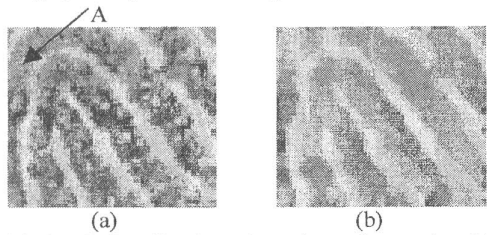


Fig.2. Median filtering of specimen fingerprint: (a) original fingerprint specimen, (b) median-filtered version of (a).

EXPERIMENTAL RESULTS

The fingerprint image was first normalised to reduce the effect of unequal finger pressure during fingerprint acquisition; which had led to low inkness in some ridge areas, making them prone to false classification. This helped to prevent the generation of false furrow regions in the binarised image (e.g point A and B in Fig 1b). After normalisation the resulting image was filtered with a median filter before global thresholding. The result of this experiment is shown as Fig.3a. This scheme wrongly classifies points A in the image as furrow whereas it is actually located on the ridge. A little perturbation in the original image around point A due to noise would result in a false ridge end (minutiae) at point A. This therefore illustrates the brittleness of such a scheme.

On the other hand, in another experiment, the fingerprint image is first histogram-equalised locally, before median filtering and finally thresholded using a global threshold. Fig.3b shows the result of this second experiment. Again this scheme wrongly classifies points B and C in the image as furrow locations whereas they are actually located on the ridges in the original specimen image, Fig.2a. Moreover, a little perturbation on at least one pixel grey value in the original image around these points, due to noise, would likely result in a false minutiae at point C in the binarised image. This also shows that this second scheme in itself is not very robust to image noise which is a typical characteristic of ink dab fingerprints especially.

In a third experiment, a combination of the two schemes mentioned above, provides an effective and reliable, ridge and furrow segmentation algorithm. In this combined scheme, a pixel is finally classified as a ridge-pixel, if it is classified as a ridge- pixel either by the procedure

in the first experiment or by the procedure described in the second experiment. Conversely, a pixel is finally classified as a furrow-pixel, only if it is classified as so by both the procedures of the schemes 1 and 2.

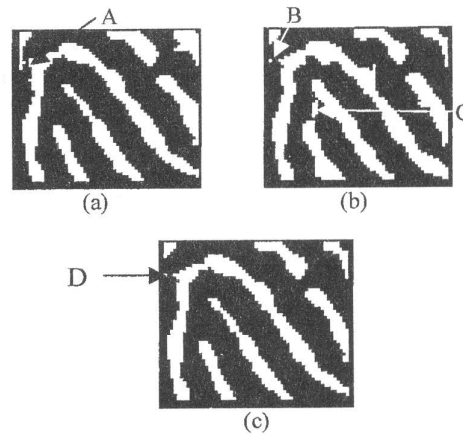


Fig.3. Median-filtering-based ridge/furrow segmentation of specimen fingerprint: (a) result of applying normalisation, median filtering and global thresholding in sequence, to the specimen fingerprint in Fig.2(a); (b) result of applying histogram equalisation, median filtering and global thresholding in sequence, to the same specimen ; (c) result of combining the schemes earlier used to obtain Fig.3(a) and Fig. 3(b) .

Fig 3c shows the result of this combined scheme as the effective ridge and furrow segmentation algorithm. The total elimination of the false furrow-pixels around point C and the small size of the surviving speckle at point B show the robustness of this last and adopted scheme to small perturbations due to noise in the fingerprint image.

However, due to the presence of noise, breaks, smudges, etc. the resulting binary ridge map often contains holes, and speckles (Hong, 1998; Jain et. al, 1997a, Jain et al, 1997b) as in point D in Fig.3c. Therefore, a hole and speckle removal algorithm is usually applied before ridge thinning. An implementation of the hole and speckle removal algorithm uses a connected component algorithm to compute the number of pixels within each ridge and each hole, and removes those connected components with numbers of pixels being less than a threshold, $T_{\text{component}}$ which in this case is 20. After the small speckles and holes are removed, a thinning algorithm can be used to generate thinned ridges with each ridges being 8-connected and single pixel in width.

Comparing the new algorithm with the one presented in Jain et al.(1997b), the new algorithm is computationally less demanding as evident from

where the right hand side of eqn. (5) is the cumulative distribution function (CDF) of r (Gonzalez, 1979).

In order to be useful for digital image processing the above concept must be formulated in discrete form. As such,

$$P_r(r_k) = \frac{n_k}{n} \quad (6)$$

where: $0 \leq r_k \leq 1$, $K = 0, 1, \dots, L - 1$, L is the number of levels, n_k is the total number of pixels at intensity level r_k and n is the total number of pixels.

The discrete form of equation (5) is given

$$S_k = T(r_k) = \sum_{j=0}^k \frac{n_j}{n} = \sum_{j=0}^k P_r(r_j) \quad (7)$$

A plot of $P_r(r_k)$ versus r_k is usually called a histogram, as such the technique used for obtaining a uniform histogram is known as histogram equalisation or histogram linearisation.

The histogram equalisation was applied locally using local windows of 11×11 pixels.

Global Thresholding

Segmentation is generally the first stage in any attempt to analyse or interpret an image automatically. Segmentation partitions an image into distinct regions that are meant to correlate strongly with objects or features of interest in the image.

Image thresholding is a segmentation technique because it classifies pixels into two categories: those at which some property measured from the image falls below a threshold, and those at which that property equals or exceeds the threshold. Since there are two possible output values, thresholding creates a binary image.

The most common form of image thresholding makes use of pixel grey level. Grey level thresholding applies to every pixel, the rule

$$g(x,y) = \begin{cases} 1, & I(x,y) \leq T \\ 0, & I(x,y) > T \end{cases} \quad (8)$$

where the aim is to detect the darker features (Efford, 2000).

A drawback to the direct application of this scheme is that it is difficult in practice except in highly constrained imaging scenarios to determine a single threshold that will always give good results through out the image. For the case of fingerprints, the singular use of basic global thresholding fails to give good results unless the fingerprint is preprocessed before its application. Hence the need for normalisation.

Fig. 1b shows the result of direct application of Global thresholding to the specimen fingerprint (Fig. 1a).

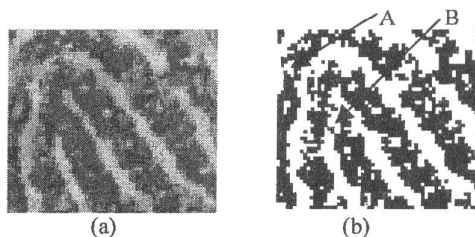


Fig.1. Direct global thresholding of a specimen fingerprint: (a) original fingerprint specimen; (b) result of application of a global threshold to the fingerprint specimen in (a).

Median Filtering

The median filter is the best-known example of a non-linear spatial filter (Gonzalez, 2000). The median filter is used to reduce speckle noise while retaining sharp edges of image features (Seul et.al, 2000). This is achieved when the intensity of the center pixel in $k \times k$ neighbourhood is replaced with the median value of the neighbouring intensities. The effect of the median filter is to replace pixel values that differ significantly from those of the other pixels in the $k \times k$ neighbourhood by the middle neighbourhood value, and this isolates neighbourhood noise very efficiently.

The median filter algorithm is as follows. Let I be the input image, I_m the filtered image, and n an odd number.

For each pixel (i, j) :

- (i) Compute the median $m(i,j)$ of the values in a $k \times k$ neighbourhood of (i, j) , $\{I(i + m, i + n), m, n \in (-k/2, k/2)\}$, where $n/2$ indicates integer division.
- (ii) Assign $I_m(i, j) = m(i, j)$ (Trucco and verri, 1998)

Ridge and Furrow Segmentation

Locally, ridges and furrows run parallel to one another forming a two-dimensional sine wave in a fingerprint image (Hong, 1998). In the case of the ink-dab fingerprints, the ridge pixels are expected to be darker (low grey levels), while the furrow pixels are expected to be lighter (high grey levels), attaining their local maximum value along a direction orthogonal to the local ridge orientation. (Jain et.al, 1997b). Unfortunately, one reason for the difficulty in segmenting ridges from furrows in a fingerprint image is that certain feature (sweat pores) present on the ridges possess similar intensity values as the valleys. As such, during pixels classification for the purpose of segmentation; if only the grey level intensity is used as a measure for differentiating a ridge pixel from a furrow pixel (eqn. 8), the sweat pore pixels

equations 1, 2 and 3. In fact, the Jain et. al. algorithm requires the computation of orientation estimates in 16×16 windows throughout the image to determine suitable value for $\theta(i,j)$ at each pixel location when applying equation 1, 2, and 3. This orientation estimation operation is a computationally demanding exercise; involving Gaussian filtering, the computation of image gradient magnitudes in both x and y directions and orientations averaging (Ratha et al., 1995; Rao, 1990 and Kass and Witkin, 1987). The new algorithm does not require orientation estimation at all. Moreover, sizes of the two convolution masks in equation 1 and 2 is given as 11×7 whereas the median filtering required in the new method utilises a small window size of at most 5×5 . On the whole, with judicious selection of a fast sorting algorithm, the new median-filtering-based approach is easier, simpler and faster to execute.

SUMMARY AND CONCLUSION

A new ridge and furrow segmentation algorithm for fingerprints has been developed. The new algorithm is a non-linear filter based method, involving an ingenious combination of normalisation, histogram equalisation, median filtering and global thresholding. The algorithm is robust to noise, even those obtainable in ink-dab fingerprints. Experimental results as evident from Figures 1, 2 and 3 show the effectiveness of the proposed algorithm. The algorithm neither requires large convolutional masks nor the initial computation of orientation estimates, as such it is faster in execution than some previous scheme.

REFERENCES

Coetzee, L. and Botha, E. C. (1993) *Fingerprint Recognition in Low Quality Images*, Pattern Recognition, vol. 26, no. 10, pp. 1441 – 1460.

Efford, N. (2000) *Digital Image Processing: a Practical Introduction Using Java*, Pearson Educational Ltd, Essex, England. pp. 251 – 253.

Gonzalez, R. C. and Wintz, P. (1979) *Digital Image Processing*, Addison-Wesley, Reading, Massachusetts, pp. 118-126.

Gonzalez, R. C. and Woods, R. E. (2002) *Digital Image Processing*, Pearson Education, Delhi, India, pp. 233-234.

Halici, U., Jain, L. C., Erol, A. (1999). Introduction to Fingerprint Recognition, In *Intelligent Biometric Techniques in Fingerprint and Face*

Recognition, Jain, L. C., Halici, U., Hayashi, I., and Lee, S. B. (Eds.), CRC Press, Boca Raton, FL, 1999, pp. 3-35.

Hong, L., *Automatic Personal Identification using Fingerprints*, Ph.D thesis, Michigan State University, USA, 1998.

Hong, L., Wan, Y. and Jain, A. (1998) Fingerprint Image Enhancement: Algorithm and Performance Evaluation, *IEEE Trans. Pattern Anal. Machine Intell.*, vol. 20, no. 8, pp. 777 – 789.

Jain, A., Hong, L. and Bolle, R. (1997a) *On-line Fingerprint Verification*, *IEEE Trans. PatternAnalysis and Machine Intelligence*, vol. 19, no. 4, pp. 302 – 314.

Jain, K. A., Hong, L., Pankanti, S. and Bolle, R. (1997b) *An Identity-Authentication System Using Fingerprints*, *Proceedings of the IEEE*, vol. 85, no. 9, pp. 1365 – 1388.

Kass, M. and Witkin, A. (1987) *Analyzing Oriented Patterns*, *Computer Vision, Graphics and Image Processing*, vol. 37, pp. 362-385.

Maio, D. and Maltoni, D. (1999) Minutiae Extraction and Filtering from Gray-Scale Images, In *Intelligent Biometric Techniques in Fingerprint & Face Recognition*, Jain, L. C., Halici, U., Hayashi, I., and Lee, S. B. (Eds.), CRC Press, Boca Raton, FL, 1999, pp. 155 – 191.

Marr, D. and Hildreth, E. C. (1980) *Theory of Edge Detection*. *Proc. R. Soc. London, B* 207, 187-217.

Miller, B. (1994) *Vital Signs of Identity*, *IEEE Spectrum*, vol. 31, no. 2, pp. 22-30.

Pal, N. R. and Pal, S. K. (1993). *A Review on Image Segmentation Techniques*. *Pattern Recognition*, vol. 26, no. 9, pp. 1277-1294.

Rao, R. A. (1990) *A Taxonomy for Texture Description and Identification*, Springer-Verlag, New York.

Ratha, K. N., Karu, K., Chen S., Jain, K. A. *A Real-Time Matching System for Large Fingerprint Databases*, *IEEE Trans. Pattern Anal. Machine Intell.*, vol 18, no. 8, pp. 799-813.

Ratha, N., Chen, S., and Jain, K. A. (1995) *Adaptive Flow Orientation Based Feature Extraction in Fingerprint Images*, *Pattern Recognition*, 28(11): 1657 – 1672.

Seul, M., O’Gorman, L., Sammon, J. M. (2000) *Practical Algorithms for Image Analysis*, Cambridge University Press, pp. 72.

Trucco, E. and Verri, A. (1998) *Introductory Techniques for 3-D Computer Vision*. Prentice Hall, N.J., USA, pp. 62.